Hydrolysis of Aliphatic *Bis*-isonitriles in the Presence of a Polar Super Aryl-Extended Calix[4]pyrrole Container

Qingqing Sun,[a][b]‡ Luis Escobar[a][b]‡ and Pablo Ballester[a][c]*

Abstract: We report binding studies of an octa-pyridinium super aryl-extended calix[4]pyrrole receptor with neutral difunctional aliphatic guests in water. The guests have terminal isonitrile and formamide groups, and the complexes display an inclusion binding geometry and 1:1 stoichiometry. Using ^{1}H NMR titrations and ITC experiments, we characterized the dissimilar thermodynamic and kinetic properties of the complexes. The *bis*-isonitriles possess independent reacting groups, however, in the presence of 1 equiv. of the receptor the hydrolysis reaction produces mixtures of non-statistical composition and a significant decrease in reaction rates. The selectivity for the *mono*-formamide product is specially enhanced in the case of the *bis*-isonitrile having a spacer with five methylene groups. The analysis of the kinetic data suggests that the observed modifications in reaction rates and selectivity are related to the formation of highly stable inclusion complexes in which the isonitrile is hidden from bulk water molecules. The concentration of the reacting substrates in the bulk solution is substantially reduced by binding to the receptor. In turn, the hydrolysis rates of the isonitrile groups for the bound substrates are slower than in the bulk solution. The receptor acts as both a sequestering and supramolecular protecting group.

Introduction

Molecular containers have been used to mediate and catalyze chemical transformations, as well as to alter the selectivity of reactions occurring in bulk solution.[1,2,3,4,5,6,7,8,9,10,11,12] In solution the *mono*-functionalization of symmetric difunctional compounds featuring independent reacting groups, *i.e.,* the chemical modification of one group has little effect on the reactivity of the other, yields statistical mixtures of products. Generally, such mixtures arising from the reaction makes the purification and isolation of the desired *mono*-reacted (non-symmetric) product challenging and troublesome. The improvement of the selectivity in desymmetrization reactions should increase their application in synthetic strategies. Molecular containers featuring non-polar cavities have been used as reaction flasks to address the *mono*-functionalization problem.[9] For example, Rebek and co-workers employed a water-soluble octa-methyl tetra-benzimidazolone resorcin[4]arene cavitand for increasing the selectivity of: the reduction of *α*,*ω*-*bis*-azides to *mono*-amines,[13] the hydrolysis of *α*,*ω*-*bis*-esters to *mono*-acids, in both acid and basic media,[14] and obtaining *mono*-epoxides from *α*,*ω*-*bis*-enes.[15] In all cases, the product distributions were exceptional, containing the *mono*-functionalized or *mono*-reacted compound in significantly larger extents than the statistically predicted upper limit (36.8%) assuming identical rate constants, $k_1 = k_2$, for each site.[14]

In these applications, the function of the molecular container doubles as supramolecular water-solubilizing and protecting group. The binding of the water-insoluble symmetric substrates to the cavitand produces soluble 1:1 inclusion complexes. The bound symmetric guests adopt folded *J*-conformations, which interconvert rapidly on the ^{1}H NMR chemical shift time scale, most likely, through a "yo-yo" motion.[16,17] The *J*-shape of the bound guest provokes an alternative exposure of only one of the two reactive ends to the bulk solution. The exposed end reacts at the interface of the inclusion complex and water. Subsequently, the equilibrium between the reacted and unreacted ends of the bound guest is modified owing to their different hydrophobicities. Typically, the unreacted site (being less polar) is preferentially hidden from the water/cavitand interface, and its further reaction is inhibited. The selectivity for the *mono*-functionalization reaction, compared to that in the absence of the container, is increased.

[a] Institute of Chemical Research of Catalonia (ICIQ), The Barcelona Institute of Science and Technology (BIST)
Av. Països Catalans, 16, 43007, Tarragona, Spain
E-mail: pballester@iciq.es
[b] Universitat Rovira i Virgili, Departament de Química Analítica i Química Orgánica
c/Marcel·lí Domingo, 1, 43007, Tarragona, Spain
[c] Catalan Institution for Research and Advanced Studies (ICREA)
Passeig Lluís Companys, 23, 08010, Barcelona, Spain
‡ These authors contributed equally.

Supporting information for this article is given via a link at the end of the document.

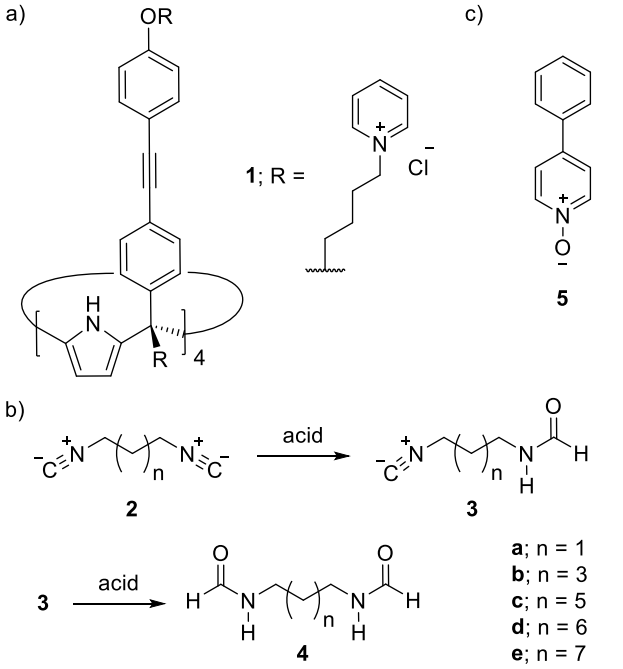

Figure 1. a) Chemical structure of SAE-C[4]P **1**; b) Stepwise reaction scheme of the acid-catalyzed hydrolysis of *bis*-isonitrile **2** to give *mono*-formamide **3** and *bis*-formamide **4**. c) Line-drawing structure of 4-phenylpyridine *N*-oxide **5** used as competitive binding guest.

The groups of Gibb,[18,19] Nitschke[20] and Dalcanale,[21] among others,[22] have also reported beautiful examples of molecular containers able to sequester reactive groups from external reagents. Both polar and steric factors have strong impacts on the transition state's energy of reactive groups sequestered in molecular containers.[23,24]

We reported the synthesis and binding properties of water-soluble aryl-extended (AE-C[4]P)[25,26] and super aryl-extended calix[4]pyrrole (SAE-C[4]P)[27] receptors containing *polar* aromatic cavities. We demonstrated that in aqueous solution an AE-C[4]P binds formamides with high affinity, $K_a > 10^4$ M^{-1}. There is selectivity for the *cis*-isomer of primary and secondary formamides,[25] despite the energetic preference for a *trans*-conformation when free in solution.[28] Water-soluble SAE-C[4]Ps were also effective in the binding of polar neutral substrates such as pyridyl *N*-oxides, $K_a > 10^5$ M^{-1}.[27] The cone conformation of AE-C[4]Ps and SAE-C[4]Ps, *i.e.,* **1** (**Figure 1**a and **Figure 3**), creates sizeable polar aromatic cavities. In water, their inclusion complexes are stabilized not only by the hydrophobic effect and CH-π, NH-π and π-π interactions[29] but also by the establishment of four convergent hydrogen bonds between the pyrrole NHs of the calix[4]pyrrole unit of the receptor and the oxygen atom of the bound guest.[30]

In bulk solution, the acid-catalyzed hydrolysis[31] of long-chain aliphatic *α,ω-bis*-isonitriles provides the *mono*-hydrolyzed formamide-isonitrile as a statistical mixture with the unreacted starting material and the doubly-hydrolyzed compound (**Figure 1**b). Formamide and isonitrile (isocyanide) functional groups display orthogonal reactivity. Isonitriles participate in multi-component reactions,[32] and are easily attached to biomolecules, making long-chain aliphatic *α,ω*-formamide-isonitriles valuable intermediates in organic and bio-organic synthesis. The efficient binding of primary formamides exhibited by water-soluble calix[4]pyrrole receptors and their supramolecular sequestering and protecting abilities suggested an improved selectivity in the hydrolysis reaction of symmetric aliphatic *α,ω-bis*-isonitriles; we report on these developments here.

Initially, we examined the binding of SAE-C[4]P **1** in water to a series of difunctional aliphatic guests: *bis*-isonitriles **2**, *mono*-formamides **3** and *bis*-formamides **4** (**Figure 1**b). We investigated the acid-catalyzed hydrolysis of a series of *bis*-isonitriles **2a**-**e** in the absence and in the presence of receptor **1** (1 equiv.). The results showed that the presence of **1** induces yield enhancements for the *mono*-formamides (non-symmetric) **3a**-**e** with respect to the statistical mixture of products obtained in the absence of the receptor. The largest yield enhancement was obtained for the *mono*-formamide **3b**. The modifications in the composition of the reaction mixture and the observed diminution in reaction rates are related to the formation of stable inclusion complexes of the reacting substrates (**2** and **3**) with receptor **1**.

Results and Discussion

The interaction of SAE-C[4]P **1** with *bis*-isonitrile **2b** and *mono*- and *bis*-formamides, **3b** and **4b**, in D_2O solution was followed using ^{1}H NMR spectroscopy (see SI). The ^{1}H NMR spectrum of a millimolar D_2O solution of free **1** shows broad proton signals due to aggregation or intermediate dynamics between conformational changes (cone and alternate). The addition of 1 equiv. of the *mono*-formamide **3b** provoked the sharpening of the signals of receptor **1**. In addition, the five methylene units of **3b** appeared upfield shifted, locating them within the four aromatic walls of SAE-C[4]P **1**. The addition of more than 1 equiv. of **3b** produced a separate set of signals corresponding to the protons of the free guest (**Figure 2**c). These results indicated the formation of a 1:1 inclusion complex, **3b**⊂**1**, for which we can estimate a stability constant value (K_a) larger than 10^4 M^{-1}, with a binding process displaying slow exchange dynamics on the ^{1}H NMR chemical shift time scale. The five methylene signals of bound **3b** showed quite different upfield shifts ($\Delta\delta < 0$), which reflect the dissimilar anisotropic shielding provided by the four walls of **1** along its aromatic cavity. In contrast to the observations made in inclusion complexes of resorcin[4]arene cavitands,[9] the magnitudes of the upfield shifts are not directly related to the various depth of the guest's alkyl chain included in the SAE-C[4]P **1**. For example, the formyl proton of bound **3b** appeared at δ = 4.39 ppm ($\Delta\delta$ = - 3.60 ppm) (see SI, **Figure S59**). We observed analogous complexation-induced shifts (CIS, $\Delta\delta$) in the binding of the *cis*-isomers of phenyl and alkyl formamides with a water-soluble AE-C[4]P.[25] This places the *cis*-formamide group of **3b** in the closed and polar aromatic cavity of calix[4]pyrrole **1**.[33] In turn, this arrangement fixes the geometry of the **3b**⊂**1** complex by placing

the isonitrile end of **3b** close to the open rim of the receptor (**Figure 3**b).

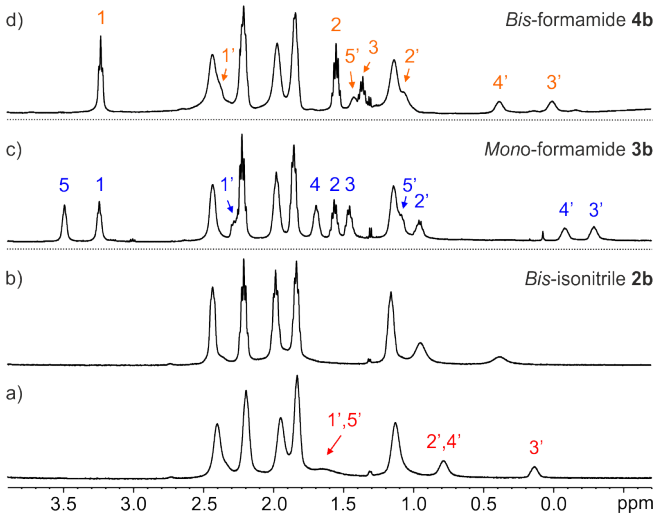

Figure 2. Selected region of the ^{1}H NMR spectra (500 MHz with cryoprobe, D_2O, 313 K) registered for the titration of SAE-C[4]P **1** with *bis*-isonitrile **2b**: a) 0.5 and b) 1 equiv. added. Panels c) and d) display the identical region of the ^{1}H NMR spectra (298 K) of mixtures containing **1** with 2 equiv. of *mono*-formamide **3b** and *bis*-formamide **4b**, respectively. Primed numbers correspond to the proton signals of bound species: **2b** (in red), **3b** (in blue) and **4b** (in orange).

The two methylene groups *alpha* (H^1) and *beta* (H^2) with respect to the formamide end of **3b** are significantly less shielded ($\Delta\delta$ = -0.99 and -0.62 ppm, respectively). This is due to their location in the cavity region of **1** surrounded by the alkynyl linkers, which impart a reduced magnetic shielding. In striking contrast, the remaining three methylene units, specially the one *alpha* to the isonitrile end (H^5), although being less deep in the cavity of **1**, experienced more intense shielding ($\Delta\delta$ = -2.42 ppm). These larger CIS derive from the placement of the methylene groups in the upper non-polar aromatic cavity of **1**. In this location, they are exposed to the strong shielding effect exerted by the four terminal phenyl substituents of the receptor.

We did not observe additional signals that could be assigned to the hydrogen atoms of the "reverse" binding geometry of the **3b⊂1** complex (**Figure 3**c). Remarkably, the chemical exchange between free and bound **3b** was fast on the EXSY time scale (t_{mix} = 0.3 s). The observed chemical exchange cross-peaks were used for unequivocal assignment of the proton signals of bound **3b**. The exclusive observation of i + 2 NOE peaks between the methylene proton signals of bound **3b** supports the extended conformation of its alkyl chain.

The binding of the symmetric *bis*-formamide **4b** with the SAE-C[4]P **1** produced identical results (see **Figure 2**d and SI for details). That is, a 1:1 inclusion complex of **4b** with $K_a > 10^4$ M^{-1}, and its slow bound/free exchange dynamics on the ^{1}H NMR chemical shift time scale. Fast exchange with the free counterpart on the EXSY time scale was detected, but not tumbling of the bound guest on the same time scale. We observed five separate signals for the methylene protons of bound **4b**. The lack of symmetry and the magnitude of the upfield shifts experienced by the methylene signals in the **4b⊂1** complex indicated that a *cis*-formamide end is bound by the calix[4]pyrrole unit of **1** while the other formamide end, in *cis* (15%) and *trans* (85%) conformation, occupies the upper non-polar aromatic cavity. We performed the assessment of the binding constant values for the **3b⊂1** and **4b⊂1** complexes using ITC experiments (**Table 1**).

A bound symmetric difunctional guest, having five methylene groups and experiencing fast tumbling on the ^{1}H NMR chemical shift time scale inside the cavity of **1**, should lead to the observation of only three signals. At 313 K, we observed only three upfield shifted signals in the ^{1}H NMR spectrum of mixtures of the symmetric *bis*-isonitrile **2b** (0.5-1 equiv.) with **1** (**Figure 2**a,b). In this case, however, the binding process displayed fast exchange dynamics on the chemical shift time scale. This latter characteristic serves to explain the symmetric pattern of the proton signals of bound **2b** without the need to invoke fast tumbling of the bound guest. The addition of more than 1 equiv. of **2b** did not induce further changes in the proton signals of **1** (**Figure S45**). This observation allows us to estimate that the binding constant value of the **2b⊂1** complex is also larger than 10^4 M^{-1}. The CIS of the methylene protons of bound **2b** were calculated by extrapolating the fit of its chemical shift changes experienced in the titration of **1** using a theoretical 1:1 binding model (**Figure S46**). The calculated values represent average chemical shifts of the two separate signals expected for both *alpha*- and *beta*-methylene protons in a **2b⊂1** complex experiencing slow dynamics on the chemical shift time scale for its binding and tumbling processes (see CIS for **2b⊂1** in **Figure 3**a). The calculated average CIS values for the two separate *alpha*- and *beta*-methylene proton signals observed for **3b⊂1** or the symmetric *bis*-formamide **4b** in the **4b⊂1** complex are in line with those of the *bis*-isonitrile **2b** in the **2b⊂1** complex. This result suggests that **2b** also adopts an extended conformation when included in the cavity of **1**. In this conformation, one of the two isonitrile groups of **2b** is more accessible to water molecules in the interface between the open end of the SAE-C[4]P **1** and the bulk solution. ITC experiments provided a more accurate value for K_a (**2b⊂1**) (**Table 1**). We calculated large and negative heat capacity values (ΔC_p) for all binding processes. This result indicates that the formation of the complexes, **2b**-**4b⊂1**, is mainly driven by the hydrophobic effect.[34,35]

Based on the above, we hypothesized that in the **2b⊂1** complex, the rate of the hydrolysis reaction producing the *mono*-formamide **3b** should be different from that in the bulk solution.

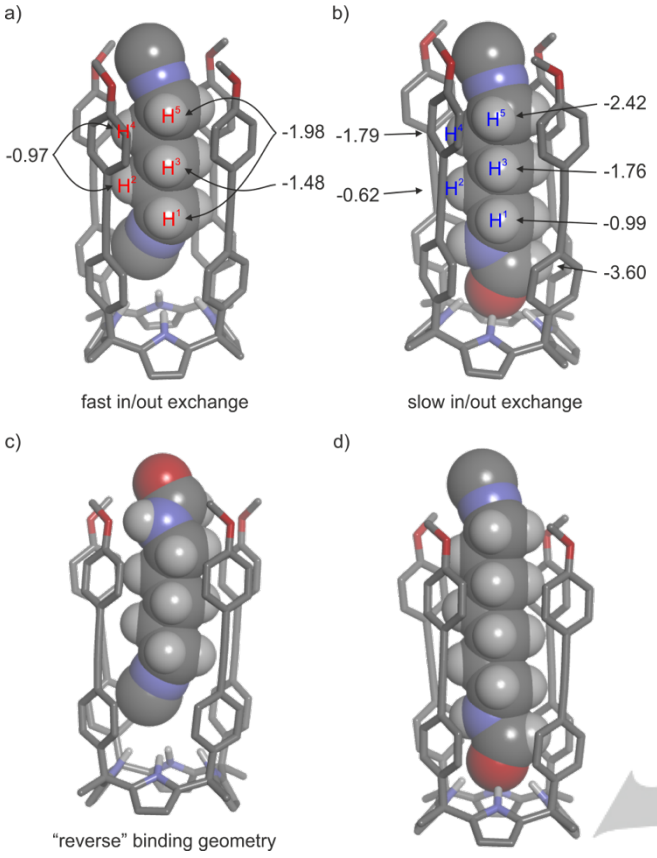

Figure 3. Gas-phase energy-minimized structures at the BP86[36,37]-Def2SVP-D3[38] level of theory of simplified 1:1 inclusion complexes: a) **2b**⊂**1**; b) **3b**⊂**1**; c) "reverse" binding geometry for **3b**⊂**1** and d) **3c**⊂**1**. The complexation-induced shifts (CIS, Δδ) experienced by all the non-polar proton signals of the bound guests, **2b** and **3b**, and the dynamics of their in/out chemical exchange process on the ^{1}H NMR chemical shift time scale are indicated. Receptor **1** is shown in line-stick representation with non-polar hydrogen atoms omitted for clarity. Bound guests are depicted as CPK models. The water-solubilizing groups at the upper and lower rims of **1** are pruned to methyl groups. See **Figure 1** for the line-drawing structures of the compounds.

Table 1. Binding constant values (K_a) determined using ITC experiments for the 1:1 complexes of receptor **1** with guests **2b**-**4b** in water at 313 K and their corresponding free energies (ΔG). Error values in K_a are reported as standard deviations and propagated to ΔG. The heat capacities (ΔC_p) were calculated using the ΔH values of ITC experiments performed at 298 and 313 K.

Guest	K_a (M^{-1}) x 10^{-5}	ΔG (kcal·mol^{-1})	ΔC_p (cal·mol^{-1}·K^{-1})
2b	1.3 ± 0.1	7.3 ± 0.1	-240
3b[a]	6.9 ± 0.9	8.3 ± 0.1	-193
4b[a]	9.2 ± 0.1	8.5 ± 0.1	-233

[a] The reported K_a values are apparent (K_{app}) because only the *cis*-isomer of the guests binds the receptor. K_a and K_{app} have similar magnitudes when the percentage of the *cis*-isomer in solution is significant, as is the case here. See reference 25 for a more detailed analysis of the ratio between these constant values.

Assuming that the reaction occurs preferentially at the water/SAE-C[4]P interface (isonitrile end located at the open cavity of the container), the resulting *mono*-formamide **3b** will locate the non-reacted isonitrile end buried in the polar cavity of **1** protected from bulk water. This would result in the "reverse" binding geometry of the **3b**⊂**1** complex (**Figure 3**c). However, as mentioned above, the ^{1}H NMR spectrum of the **3b**⊂**1** complex (**Figure 2**c) did not show additional proton signals hinting to the presence of this isomer in solution. Nevertheless, we cannot rule out its existence to a reduced extent (< 10^{-4} M). Our expectations were that the inclusion of the *bis*-isonitrile **2b** and the *mono*-formamide **3b** in the cavity of **1** might produce a reduction in the hydrolysis reaction rates of their isonitrile ends exposed at the water/container interface in comparison to the bulk solution. Possible reasons of this putative effect include: a limited exposure to bulk water molecules and a reduced solvation of the transition state. It is worth mentioning that the superior binding properties of SAE-C[4]P **1** for the *mono*-formamide **3b** will reduce its concentration in solution to a large extent.[39]

In order to test our hypotheses, we studied the hydrolysis reaction of *bis*-isonitrile **2b** chaperoned by the synthetic container **1** in water. In doing so, we also wanted to evaluate the potential application of **1** in addressing the *mono*-functionalization problem of **2b**. We performed the hydrolysis reaction by adding 5 equiv. of citric acid as a solution (0.5 M in D_2O) to a NMR tube containing an equimolar mixture (1 mM) of **2b** and **1** in 0.5 mL of D_2O (final pD ~ 3). We monitored the progress of the reaction at 313 K using ^{1}H NMR spectroscopy (see SI, **Figure S129**). The distribution of the species as a function of time was determined using the integral values of the methylene proton signals in the corresponding inclusion complexes. [40] Alternatively, we added 1.2 equiv. of 4-phenylpyridine *N*-oxide **5** (**Figure 1**c) to the reaction mixture at different time intervals (**Figure S132**). *N*-oxide **5** is a competitive guest[27] that displaces the reacting species bound in the cavity of **1** to the bulk solution. Next, we used the integral values of the proton signals of the displaced guests to determine their concentrations. The two methodologies produced similar results.

The formation of the *mono*-formamide **3b** was evident from the loss of symmetry of its inclusion complex. Please note that we assigned a preferred binding geometry for the **3b**⊂**1** complex fixing the formamide group in the calix[4]pyrrole unit and having an extended conformation for the alkyl spacer (*vide supra*). After *ca.* 2 h, the composition of the reaction mixture contained the *mono*-formamide **3b** in an amount close to 80% (**Figure 4**a). This result suggests that the remaining isonitrile group in the **3b**⊂**1** complex is less accessible to bulk water. It also represents a significant improvement of the theoretical 36.8% predicted by Rebek and co-workers in the *mono*-functionalization of symmetrical difunctional substrates having independent reacting groups.[14] The isolation of the *mono*-formamide **3b** was possible by extracting it from the neutralized aqueous solution using ethyl acetate (**Figure S139**).

In analogy to the Rebek's report,[14] we fit the experimental concentration data *vs* time to a theoretical kinetic model of two

consecutive first-order irreversible reaction steps, Eqs. 1 and 2 (model 1), using COPASI kinetic modeling software.

$$\mathbf{2b}\subset\mathbf{1} \xrightarrow{k_1} \mathbf{3b}\subset\mathbf{1} \quad (1)$$

$$\mathbf{3b}\subset\mathbf{1} \xrightarrow{k_2} \mathbf{4b}\subset\mathbf{1} \quad (2)$$

From the fit of the data, we obtained the rate constant values k_1 = 1.7 x 10^{-2} min^{-1} and k_2 = 2.3 x 10^{-3} min^{-1} (**Figure 4**a, dashed lines). Based on this model, the determined rate constant values for the hydrolysis reactions in the water/container interface show that the first step (Eq. 1) is seven-fold faster than the second one (Eq. 2). This result is difficult to reconcile with the experimental observation made for the **3b**⊂**1** complex, which preferentially locates the reactive isonitrile end at the open cavity of the container not providing an increased protection for its hydrolysis.

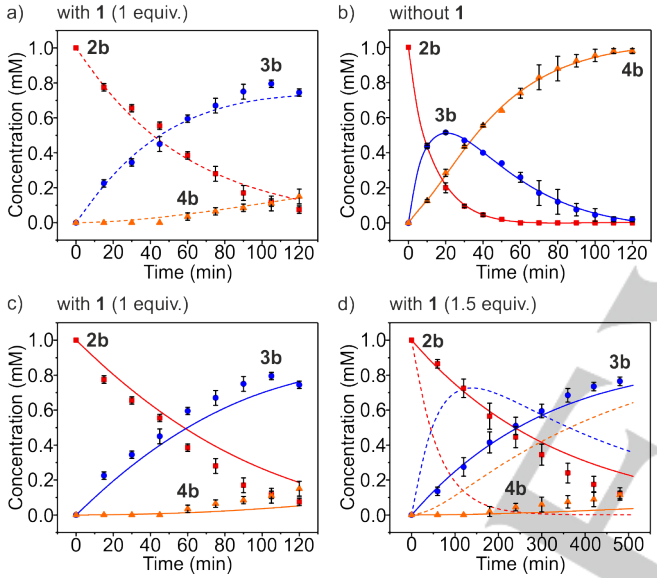

Figure 4. Plots of the concentration of the species *vs* time for the acid-catalyzed hydrolysis of *bis*-isonitrile **2b**: a) with 1 equiv. of **1**; b) without container; c) with 1 equiv. of **1** and d) with 1.5 equiv. of **1**. Dashed lines represent fit/simulation of the kinetic data to model 1 in a) and d). Solid lines represent fit/simulation of the kinetic data to model 2 in b) and model 3 in c) and d). Error bars are standard deviations.

Moreover, model 1 disregards that the reactions can also take place in the bulk solution by assuming that the rates are very slow and the concentration of the free substrates negligible. However, the *bis*-isonitrile **2b** and the *mono*-formamide **3b** are perfectly soluble in water at millimolar concentrations.

Using identical conditions, we performed the hydrolysis experiment of the *bis*-isonitrile **2b** in the absence of container **1**. The reaction profile showed also a good fit to two consecutive first-order irreversible reactions, Eqs. 3 and 4 (model 2), with k_3 = 7.0 x 10^{-2} min^{-1} and k_4 = 3.5 x 10^{-2} min^{-1} (**Figure 4**b, solid lines).

$$\mathbf{2b} \xrightarrow{k_3} \mathbf{3b} \quad (3)$$

$$\mathbf{3b} \xrightarrow{k_4} \mathbf{4b} \quad (4)$$

The selectivity of the reaction for the *mono*-formamide **3b** reached a maximum of 50%, in agreement with the theoretical statistical distribution for identical microscopic reaction rate constants. As could be expected from a protective/sequestering effect of the container, the calculated rate constant values in the absence of **1** increased more than four-fold with respect to those determined above. For this reason, the 50% maximum concentration of **3b** was obtained after 20 min of reaction compared to *ca.* 2 h needed to produce **3b** in an extent of 80% in the presence of **1**.

Having determined the rate constants for the hydrolysis reaction of **2b** in the bulk solution and the binding constants of the inclusion complexes of **1** with all the species at 313 K, we decided to mathematically analyze the hydrolysis data in the presence of **1** using a more elaborate kinetic model. This model includes two consecutive irreversible reactions occurring in the bulk solution, Eqs. 3 and 4, and the reversible formation of three complexes: **2b**⊂**1**, **3b**⊂**1** and **4b**⊂**1**, Eqs. 5-7 (model 3). It also assumes that the rates of the hydrolysis reaction of the bound substrates are negligible.

$$\mathbf{2b} + \mathbf{1} \underset{}{\overset{K_a(\mathbf{2b}\subset\mathbf{1})}{\rightleftharpoons}} \mathbf{2b}\subset\mathbf{1} \quad (5)$$

$$\mathbf{3b} + \mathbf{1} \underset{}{\overset{K_a(\mathbf{3b}\subset\mathbf{1})}{\rightleftharpoons}} \mathbf{3b}\subset\mathbf{1} \quad (6)$$

$$\mathbf{4b} + \mathbf{1} \underset{}{\overset{K_a(\mathbf{4b}\subset\mathbf{1})}{\rightleftharpoons}} \mathbf{4b}\subset\mathbf{1} \quad (7)$$

Fixing k_3 and k_4 to the values determined in the absence of **1**, and K_a (**2b**⊂**1**), K_a (**3b**⊂**1**) and K_a (**4b**⊂**1**) to the measured magnitudes (**Table 1**), within experimental error, also produced a reasonable fit to the experimental distribution of the species for the time course of the hydrolysis reaction of **2b** chaperoned by **1** (**Figure 4**c, solid lines).

Remarkably, the theoretical kinetic models 1 and 3 produced quite different results in the simulations of the time course for the hydrolysis reaction of **2b** chaperoned by 1.5 equiv. of **1**. Model 1 considers that the hydrolysis reactions take place exclusively in the bound substrates and forecasts no changes in reaction rates.[41] Conversely, model 3 assuming that only the free species are hydrolyzed in the bulk aqueous solution projects a significant reduction in reaction rates owing to the increased sequestering effect of the free reacting species by complexation with the additionally added container.

In order to evaluate which of the two models was most reliable, we experimentally undertook the hydrolysis of **2b** in the presence of 1.5 equiv. of **1**. **Figure 4**d displays the experimental time course of the reaction (points). The dashed and solid lines represent the simulated kinetic profiles using models 1 and 3, respectively. The simulation of the experimental data to model 3 is good, suggesting that it better explains the observed selectivity enhancement in the acid-catalyzed hydrolysis of **2b**. In short, container **1** sequesters **2b** and **3b** offering protection to their isonitrile end groups towards the hydrolysis reaction. The hydrolysis of the substrates occurs mainly as the free species present in the bulk solution. Because the concentrations of the free reactants are very low, their hydrolysis reaction rates are reduced. This is specially the case for the *mono*-formamide **3b**,

whose concentration free in solution becomes relevant when close to 80% of **2b** has reacted.

To evaluate the scope and generality of the sequestering and protection effect delivered by the synthetic chaperone **1** in improving the selectivity for the acid-catalyzed hydrolysis of symmetric aliphatic *α*,*ω*-*bis*-isonitriles, we used a series of shorter and longer homologues of **2b** (**Figure 1**b). In the case of the *bis*-isonitrile **2a**, having a spacer with three methylene groups, the reaction selectivity for the *mono*-formamide **3a** was reduced to 70% and the reaction rate was just slightly diminished compared to that in the absence of **1**. The maximum percentage of **3a** was obtained after 40 min of reaction instead of *ca.* 2 h required for **3b**. Taking into account the smaller binding affinities of the shorter substrates **2a** and **3a** for **1** (see SI), compared to the longer counterparts **2b** and **3b**, the obtained results can be simply explained by invoking an attenuation in the sequestering effect of the container. Also in this case, model 3 provides a good fit to the obtained hydrolysis kinetic data (see SI, **Figure S128**).

Longer *bis*-isonitriles **2c**-**e**, having seven to nine methylene groups as spacers, and their corresponding *mono*-formamides **3c**-**e** (**Figure 1**b) display higher affinity for receptor **1** (**Tables S12** and **S13**). As mentioned above, the hydrophobic effect is an important component in the binding of the homologous series of difunctional aliphatic guests by **1**. The selectivity of the *mono*-formamides **3c**-**e** in the hydrolysis reactions of **2c**-**e** (1% DMSO/D_2O)[42] reaches values of 55-65%. The achievement of these selectivities require extensive reaction times (3 – 8 h). On the other hand, the hydrolysis reactions of **2c**-**e** in the absence of **1** (see SI) produced similar results to those discussed above for **2b**.[43] Taking together, these results suggest that the longer symmetric difunctional substrates being more hydrophobic are present in reduced concentrations in the bulk solution. On the other hand, the formed inclusion complexes with **1** might provide a decrease in the hydrolysis rate of the bound isonitrile end group that is located close to the open cavity of the container but not inhibition (total protection). This is due to the increased protrusion of the isonitrile end groups of these complexes into the water/container interface (see **Figure 3**d for the energy-minimized structure of the **3c**⊂**1** complex).

Conclusions

In summary, we demonstrated that, in water solution, the octa-pyridinium SAE-C[4]P **1** forms highly stable 1:1 inclusion complexes with a series of symmetric and non-symmetric difunctional aliphatic guests: *bis*-isonitriles, *bis*-formamides and formamide-isonitriles. The *cis*-conformation of the formamide end group is preferentially included in the deep aromatic cavity of **1**. Four hydrogen bonds are established between the oxygen atom of the *cis*-formamide and the four pyrrole NHs of the calix[4]pyrrole unit of **1**. The large and negative heat capacity values measured for the complexation processes indicate that the hydrophobic effect is important for binding. Remarkably, the CIS experienced by the methylene groups in the bound guests are not related to its depth in the aromatic cavity of **1**. The addition of 1 equiv. of container **1** to the acid-catalyzed hydrolyses of the *bis*-isonitriles modifies the reaction selectivity towards the *mono*-formamides and the reaction rates compared to those in the bulk aqueous solution. The mathematical analysis of the kinetic data suggests that the influence of the container **1** is mainly related to sequestration, due to complexation, of the reacting substrates from solution. In addition, the hydrolysis reaction of the isonitrile group in the bound substrates occurs with rate constants that are smaller than in solution. The protection level offered by **1** to the hydrolysis reaction of the bound guests depends on their length. For substrates having a spacer of five methylene groups (**2b** and **3b**), their hydrolysis reaction seems to be inhibited in the bound state. The right combination of binding affinity and protection offered by **1** leads, after *ca.* 2 h of reaction time, to a maximum of 80% selectivity for the *mono*-formamide **3b** in the hydrolysis of the *bis*-isonitrile **2b**. To the best of our knowledge, the effect exerted by a synthetic container, featuring a polar aromatic cavity (**1**), on the chemical selectivity of a desymmetrization reaction in water solution and its proposed function mechanism are unprecedented.[44]

Experimental Section

Experimental procedures and characterization data of the synthesized compounds, NMR titration spectra, ITC experiments, plots of the kinetic data for the hydrolysis reactions, protocols used in the GC-FID analyses of the reaction mixtures and energy-minimized structures of selected inclusion complexes are contained in the Supporting Information for this article.

Acknowledgements

We thank Gobierno de España MCIN/AEI/FEDER, UE (projects CTQ2017-84319-P and CEX2019-000925-S), the CERCA Programme/Generalitat de Catalunya, and AGAUR (2017 SGR 1123) for financial support. Q. S. thanks the Chinese Research Council for a predoctoral fellowship (2017-06870013). L. E. thanks MECD for a predoctoral fellowship (FPU14/01016).

Keywords: Amides • Host-Guest Systems • Isonitriles • Molecular Containers • Mono-Functionalization

[1] J. Kang, J. Rebek, *Nature* **1997**, *385*, 50-52.
[2] M. Yoshizawa, M. Tamura, M. Fujita, *Science* **2006**, *312*, 251-254.
[3] M. D. Pluth, R. G. Bergman, K. N. Raymond, *Science* **2007**, *316*, 85-88.
[4] V. Ramamurthy, *Acc. Chem. Res.* **2015**, *48*, 2904-2917.
[5] W. Cullen, M. C. Misuraca, C. A. Hunter, N. H. Williams, M. D. Ward, *Nat. Chem.* **2016**, *8*, 231-236.

[6] A. Palma, M. Artelsmair, G. L. Wu, X. Y. Lu, S. J. Barrow, N. Uddin, E. Rosta, E. Masson, O. A. Scherman, *Angew. Chem., Int. Ed.* **2017**, *56*, 15688-15692.
[7] C. M. Hong, R. G. Bergman, K. N. Raymond, F. D. Toste, *Acc. Chem. Res.* **2018**, *51*, 2447-2455.
[8] N. W. Wu, I. D. Petsalakis, G. Theodorakopoulos, Y. Yu, J. Rebek, *Angew. Chem., Int. Ed.* **2018**, *57*, 15091-15095.
[9] Y. Yu, J. Rebek, Jr., *Acc. Chem. Res.* **2018**, *51*, 3031-3040.
[10] K. Wang, X. Cai, W. Yao, D. Tang, R. Kataria, H. S. Ashbaugh, L. D. Byers, B. C. Gibb, *J. Am. Chem. Soc.* **2019**, *141*, 6740-6747.
[11] H. Takezawa, T. Kanda, H. Nanjo, M. Fujita, *J. Am. Chem. Soc.* **2019**, *141*, 5112-5115.
[12] H. Takezawa, K. Shitozawa, M. Fujita, *Nat. Chem.* **2020**, *12*, 574-578.
[13] D. Masseroni, S. Mosca, M. P. Mower, D. G. Blackmond, J. Rebek, *Angew. Chem., Int. Ed.* **2016**, *55*, 8290-8293.
[14] Q. X. Shi, M. P. Mower, D. G. Blackmond, J. Rebek, *Proc. Natl. Acad. Sci. U. S. A.* **2016**, *113*, 9199-9203.
[15] V. Angamuthu, F.-U. Rahman, M. Petroselli, Y. Li, Y. Yu, J. Rebek, *Org. Chem. Front.* **2019**, *6*, 3220-3223.
[16] K. D. Zhang, D. Ajami, J. V. Gavette, J. Rebek, *J. Am. Chem. Soc.* **2014**, *136*, 5264-5266.
[17] Y.-S. Li, L. Escobar, Y.-J. Zhu, Y. Cohen, P. Ballester, J. Rebek, Y. Yu, *Proc. Natl. Acad. Sci. U. S. A.* **2019**, *116*, 19815-19820.
[18] S. Liu, H. Gan, A. T. Hermann, S. W. Rick, B. C. Gibb, *Nat. Chem.* **2010**, *2*, 847-852.
[19] K. Wang, J. H. Jordan, B. C. Gibb, *Chem. Commun.* **2019**, *55*, 11695-11698.
[20] M. M. J. Smulders, J. R. Nitschke, *Chem. Sci.* **2012**, *3*, 785-788.
[21] R. M. Yebeutchou, E. Dalcanale, *J. Am. Chem. Soc.* **2009**, *131*, 2452-2453.
[22] A. Galan, P. Ballester, *Chem. Soc. Rev.* **2016**, *45*, 1720-1737.
[23] P. Mal, B. Breiner, K. Rissanen, J. R. Nitschke, *Science* **2009**, *324*, 1697-1699.
[24] C. M. Hong, M. Morimoto, E. A. Kapustin, N. Alzakhem, R. G. Bergman, K. N. Raymond, F. D. Toste, *J. Am. Chem. Soc.* **2018**, *140*, 6591-6595.
[25] L. Escobar, A. Diaz-Moscoso, P. Ballester, *Chem. Sci.* **2018**, *9*, 7186-7192.
[26] G. Peñuelas-Haro, P. Ballester, *Chem. Sci.* **2019**, *10*, 2413-2423.
[27] L. Escobar, P. Ballester, *Org. Chem. Front.* **2019**, *6*, 1738-1748.
[28] V. P. Manea, K. J. Wilson, J. R. Cable, *J. Am. Chem. Soc.* **1997**, *119*, 2033-2039.
[29] L. M. Salonen, M. Ellermann, F. Diederich, *Angew. Chem., Int. Ed.* **2011**, *50*, 4808-4842.
[30] B. Verdejo, G. Gil-Ramirez, P. Ballester, *J. Am. Chem. Soc.* **2009**, *131*, 3178-3179.
[31] Y. Y. Lim, A. R. Stein, *Can. J. Chem.* **1971**, *49*, 2455-2459.
[32] H. Stockmann, A. A. Neves, S. Stairs, K. M. Brindle, F. J. Leeper, *Org. Biomol. Chem.* **2011**, *9*, 7303-7305.
[33] The observation of a cross-peak in the ROESY NMR spectrum between the formyl proton included in the calix[4]pyrrole unit and the corresponding *alpha*-methylene protons supports the *cis*-conformation of the buried formamide group.
[34] N. V. Prabhu, K. A. Sharp, *Annu. Rev. Phys. Chem.* **2005**, *56*, 521-548.
[35] L. Escobar, P. Ballester, *Chem. Rev. (Washington, DC, U. S.)* **2021**, DOI: 10.1021/acs.chemrev.0c00522.
[36] J. P. Perdew, *Phys. Rev. B* **1986**, *33*, 8822-8824.
[37] A. D. Becke, *Phys. Rev. A* **1988**, *38*, 3098-3100.
[38] S. Grimme, J. Antony, S. Ehrlich, H. Krieg, *J. Chem. Phys.* **2010**, *132*, 154104.
[39] M. Petroselli, V. Angamuthu, F.-U. Rahman, X. Zhao, Y. Yu, J. Rebek, *J. Am. Chem. Soc.* **2020**, *142*, 2396-2403.
[40] If all binding constant values of the complexes have similar magnitudes (see **Table 1**), this methodology can be used to calculate the total concentration of the reacting species (free + bound) because their distribution is reflected by the relative concentrations of the complexes.
[41] The simulation of the time course for the hydrolysis reaction of **2b** in the presence of 1.5 equiv. of **1** using a kinetic model composed of Eqs. 1, 2, 5, 6 and 7 produced a similar result to that obtained using model 1.
[42] The hydrolysis reaction of longer *bis*-isonitriles **2c**-**e** in the presence of container **1** was performed in 1% DMSO/D_2O due to solubility reasons.
[43] Due to the overlap of proton signals and reduced solubility, we used GC-FID to monitor the reaction kinetics in the control hydrolysis experiments of the longer *bis*-isonitriles **2c**-**e**. The addition of 1% of DMSO did not produce a modification of the maximum selectivity of the *mono*-formamide.
[44] Previous reports on the use of molecular containers in controlling the selectivity of desymmetrization reactions in water made exclusive use of non-polar binding cavities.

Entry for the Table of Contents (Please choose one layout)

Layout 1:

FULL PAPER

A super aryl-extended calix[4]pyrrole acts as both a sequestering and supramolecular protecting group, enhancing the selectivity for the *mono*-formamide product in the hydrolysis of aliphatic *bis*-isonitriles.

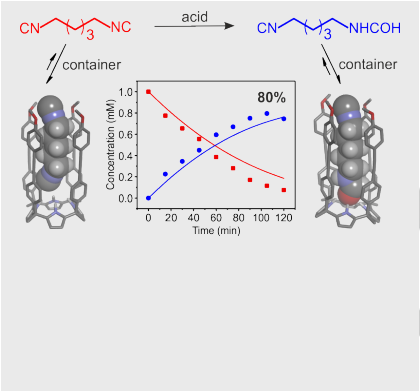

*Qingqing Sun, Luis Escobar and Pablo Ballester**

Page No. – Page No.

Hydrolysis of Aliphatic *Bis*-isonitriles in the Presence of a Polar Super Aryl-Extended Calix[4]pyrrole Container

Layout 2:

FULL PAPER

((Insert TOC Graphic here; max. width: 11.5 cm; max. height: 2.5 cm))

*Author(s), Corresponding Author(s)**

Page No. – Page No.

Title

Text for Table of Contents